applied sciences

MDPI

Article

Development of a Web Application for the Detection of Coronary Artery Calcium from Computed Tomography

Juan Aguilera-Alvarez [1], Juan Martínez-Nolasco [2,*], Sergio Olmos-Temois [3], José Padilla-Medina [4], Víctor Sámano-Ortega [1] and Micael Bravo-Sanchez [1]

[1] Doctorado en Ciencias de la Ingeniería, Tecnológico Nacional de México/IT de Celaya, Celaya 38010, Mexico
[2] Departamento de Ingeniería Mecatrónica, Tecnológico Nacional de México/IT de Celaya, Celaya 38010, Mexico
[3] Departamento de Cardiología, Centro Médico Quirúrgico, Celaya 38000, Mexico
[4] Departamento de Ingeniería Electrónica, Tecnológico Nacional de México/IT de Celaya, Celaya 38010, Mexico
* Correspondence: juan.martinez@itcelaya.edu.mx

Abstract: Coronary atherosclerosis is the most common form of cardiovascular diseases, which represent the leading global cause of mortality in the adult population. The amount of coronary artery calcium (CAC) is a robust predictor of this disease that can be measured using the medical workstations of computed tomography (CT) equipment or specialized tools included in commercial software for DICOM viewers, which is not available for all operating systems. This manuscript presents a web application that semiautomatically quantifies the amount of coronary artery calcium (CAC) on the basis of the coronary calcium score (CS) using the Agatston technique through digital image processing. To verify the correct functioning of this web application, 30 CTCSs were analyzed by a cardiologist and compared to those of commercial software (OsiriX DICOM Viewer).All the scans were correctly classified according to the cardiovascular event risk group, with an average error in the calculation of CS of 1.9% and a Pearson correlation coefficient r = 0.9997, with potential clinical application.

Keywords: Agatston score; computed tomography; coronary artery calcium; image processing; web application

Citation: Aguilera-Alvarez, J.; Martínez-Nolasco, J.; Olmos-Temois, S.; Padilla-Medina, J.; Sámano-Ortega, V.; Bravo-Sanchez, M. Development of a Web Application for the Detection of Coronary Artery Calcium from Computed Tomography. *Appl. Sci.* **2022**, *12*, 12281. https://doi.org/10.3390/app122312281

Academic Editors: Jing Zhang, Jipeng Qiang and Cangqi Zhou

Received: 4 November 2022
Accepted: 28 November 2022
Published: 30 November 2022

1. Introduction

The World Health Organization indicates that 17.9 million people died from cardiovascular diseases in 2019, which represent 32% of all deaths worldwide [1]. Atherosclerosis is a progressive disease characterized by the accumulation of lipids and fibrous elements in the large arteries, and it is the primary cause of heart disease and stroke [2]. Atherosclerosis is closely related to the calcified plaque detected in coronary arteries [3,4], which is known as coronary artery calcium (CAC), and its detection is considered to be one of the strongest indicators to predict the presence of atherosclerosis in patients who do not have symptoms yet [5–7]. The most common way to detect CAC is through a cardiac computed tomography (CT) for calcium scoring (CTCS), which consists of a noncontrast enhanced CT of the heart [8], which is interpreted by quantifying the coronary calcium score (CS) in terms of the Agatston score [9–11]. CS is determined on CTCS by identifying calcified lesions that are represented on CT as pixel islands with an intensity greater than 130 Hounsfield units (HU) belonging to one of the coronary arteries: left main (LM), left anterior descending (LAD), circumflex (CX), and right coronary artery (RCA) [9].

Digital image processing provides techniques frequently used in the identification of CAC, for example, the design of automatic algorithms to obtain CS, the segmentation of coronary arteries, and the relationship between other clinical indicators and CAC. For the development of these studies, some researchers use open-source medical image processing software such as 3DSlicer [12] to manually segment lesions or regions of interest (ROIs); the manually obtained information is supplied to computed or statistical systems for analysis and/or interpretation [13–15]. Another open-source software option is ImageJ [16], which, in addition to allowing for manual operations with images, allows for developers to use predefined semiautomatic functions and the possibility of creating custom macros or plugins to automate some image process analyses [17–21]. An alternative to the previously defined software is the use of the OpenCV open-source library [21] which allows for implementing more complete image processing techniques through predefined classes and functions [22–25].

The development of applications with web technology has increased significantly because they present advantages such as (1) no installation required, (2) automatic updates, and (3) universal access form any device connected to the internet [26]. Web applications have been developed in medicine [27–29] especially during COVID-19 [30–32] , academia [33,34], ecology [35,36], and biology [37,38], among others [39–41]. This article presents a web application to determine the CAC on the basis of the Agatston score evaluated with digital processing techniques in the corresponding images included in a CTCS.

2. Materials and Methods

The web application uses CTCS scans to perform the semiautomatic calculation of the CS in the lesions defined by the specialist in cardiovascular medicine. Its implementation required three stages: (1) image processing and the calculation of results, (2) the programming of the web page, and (3) the deployment of the application on the Internet (Figure 1). The backend was programmed in the Python language, and the frontend was developed with the HTML, CSS, and JavaScript languages. The web application was mounted onto a virtual private server (VPS), so that users could use it from any device with an Internet connection. A physician with a specialty in cardiology and 10 years of experience in the field compared the results of the web application with the results of the OsiriX DICOM Viewer software, which is the application that the cardiologist uses daily. Two filters were proposed to remove noise from to the image, so three CS values were evaluated, Pearson's correlation coefficient was calculated for each of the assessments performed in comparison with the reference OsiriX DICOM viewer software, and the diagnoses issued by the specialist were also compared with the total CS value per scan for each developed method. Lastly, the risk of a. cardiovascular event corresponding to each of the studies according to the classification given by the CS was compared with the reference.

2.1. Calculation of the Coronary Calcium Score

For the calculation of CS in the coronary arteries, the calcified lesions represented on the CT as pixel islands with intensity greater than 130 HU located in one of the four coronary arteries (LM, LAD, CX, and RCA) are identified. Figure 2 shows an example of a lesion of each of the ROIs identified with different colors (LM: red, LAD: blue, CX: yellow, and RCA: green). In addition, pixel islands with an intensity greater than 130 HU are shown that were not part of any of the coronary arteries (such as bones); these islands were identified as None (cyan).

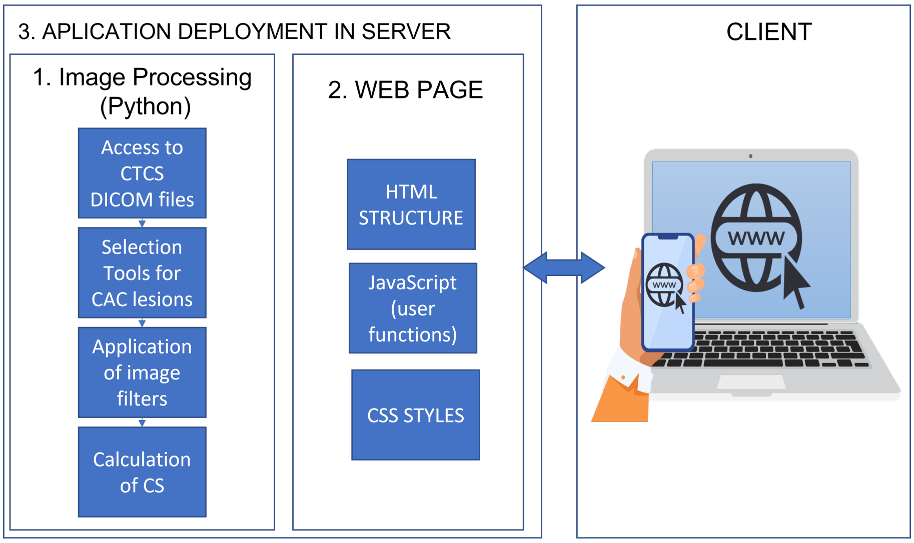

Figure 1. Stages of web application development.

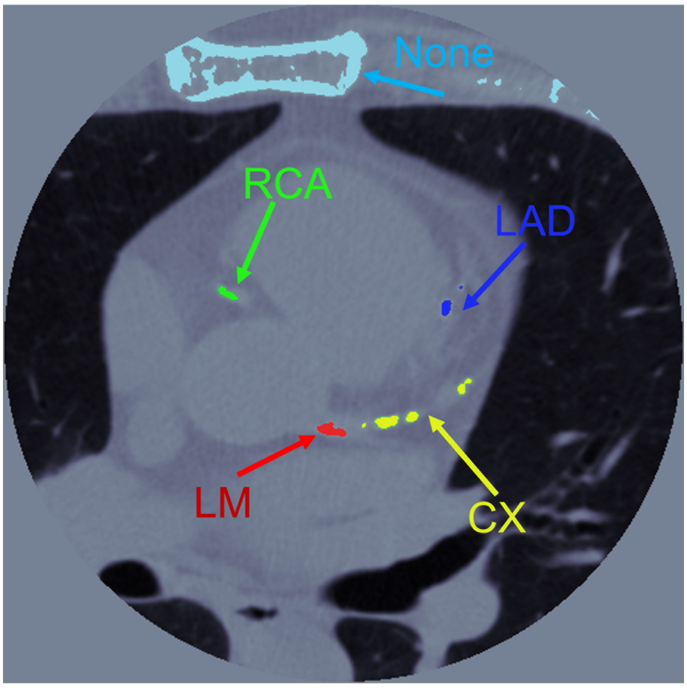

Figure 2. Example of islands of pixels with an intensity greater than 130 HU and their labels.

The CS in terms of the Agatston score is an indicator of the presence of coronary artery disease (CAD) and determines the presence of atherosclerosis in patients who do not even have symptoms [5–7].

To calculate the Agatston score, the density score (F) is used, which depends directly on the maximal HU value of the lesion. The possible values of F are (a) F = 1 if 130 $\leq HUmax \leq 199$, (b) F = 2 if 200 $\leq HUmax \leq 299$, (c) F = 3 if 300 $\leq HUmax \leq 399$, (d) F = 4 if 400 $\leq HUmax$ [9]. In addition, the area (a) of the calcified lesion in mm^2 was evaluated. Equation (1) was used to evaluate the CS, where n represents the number of lesions.

$$CS = \sum_{i=1}^{n} F_1 \times a_1 \quad (1)$$

In the calculation of CS, islands of pixels with an area of less than 1 mm^2 were not considered because it was established as such in the medical protocol [9].

2.2. Image Dataset

The dataset was integrated with 80 CTCS scans obtained in three hospitals that had different tomographic equipment. This implies that each scan has a different pixel area measurement that is obtained from the header of the DICOM file, and all images were reconstructed to 2.5 mm slice thickness. In the conformation of the database, 30 scans (Hospital 1: 15 scans, Hospital 2: 9 scans, Hospital 3: 6 scans) were chosen to have a representative sample of each cardiovascular event risk group: moderate ($10 < CS \leq 100$),, moderate–high ($100 < CS \leq 400$), and high ($CS > 400$), the former due to the fact that they presented a greater number of lesions per scan, obtaining more information compared to the groups of very low ($CS = 0$) or low ($0 < CS \leq 10$) in which the number of pixel islands is minimal. To calculate the CS, the web application accesses the tags from the DICOM files: (1) 0028,000A—columns, (2) 0028,0010—rows, (3) 0028,0030—pixel spacing, (4) 0028,0102—high bit, (5) 0028,1052—rescale intercept. No patient name or other information is necessary, so anonymous scans are possible to load.

2.3. Image Processing

In this stage, the Pydicom and OpenCV Python libraries are used. With Pydicom [42], DICOM files with information compatible to Python were integrated. With the OpenCV library [43], conversion, binarization and filtering operations were performed on the images obtained from Pydicom. To evaluate the CS, the lesions of each slice of the CTCS scan were selected; consequently, the image processing algorithm performs the following functions (Figure 3): (1) open the image set and navigate through the slices, (2) identify pixel areas greater than 130 HU, (3) select lesions of calcium in the arteries, adding labels according to the corresponding coronary artery (LAD, LM, CX, and RCA). The original image is represented in HU and is converted into a grayscale map, so that the user can easily identify the elements that comprise the CT image (Grayscale). Later, this image is represented in RGB format to obtain an image with color. With the original image (HU), two binary images are also generated. In the first, pixels with HU values greater than or equal to 130 HU are labeled with a "1", and in the second, pixels with HU values less than 130 HU are labeled "1". From the image with pixels ≥ 130 HU, an image (Labeling) with islands of labeled pixels is obtained that is used to obtain information that allows for finding the relationship between possible lesions and the corresponding coronary artery (Selected Calcifications). To obtain the image that is shown to the user (Final Image), areas greater than 130 HU are extracted from the RGB image, and the result is added to the Selected Calcifications image.

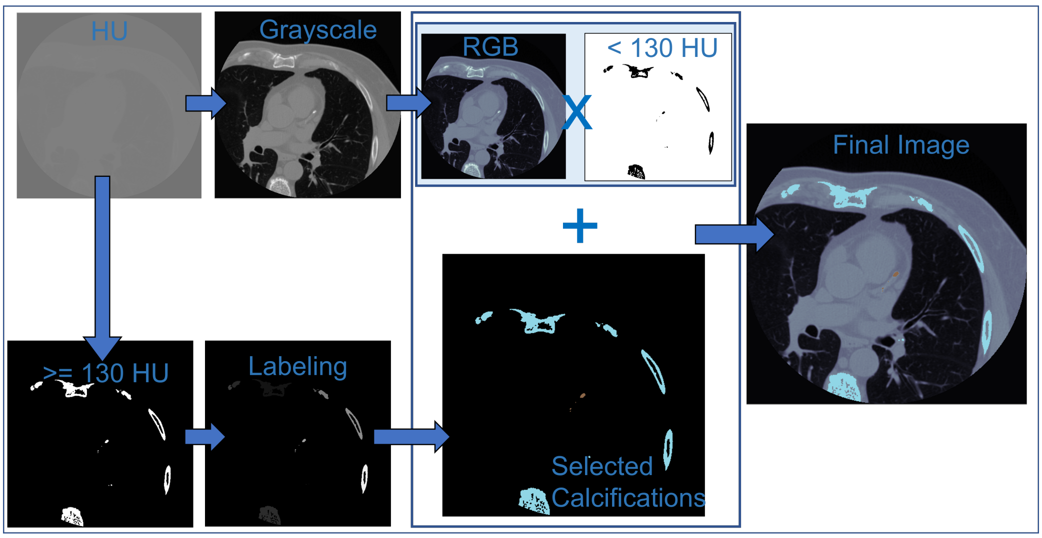

Figure 3. Digital processing of computed tomography images.

Each time the user points to a pixel island (Figure 4), it is labeled with the selected coronary artery (LAD, LM, CX and RCA), saving the relationship of each of the lesions in a Python list and changing the color of the island of pixels by that corresponding to the artery. The application calculates the area of the selected lesion. If the area is greater than or equal to 1 mm^2, the corresponding density score is calculated. Since there may be variations in the CTCS due to the size of the patient and the calibration of the tomographic equipment, increasing the final value of the CS [44], the application of two additional processing techniques for the attenuation of the variations was proposed, and three different density scores were calculated. The first density score (F1) corresponds to the selected island of pixels as proposed by Agatston [9]. The second proposed density score (F2) is calculated after the application of a Gaussian blur filter that was programmed with the GaussianBlur function that is included in the OpenCV library. The third proposed density score (F3) is calculated after applying a classification criterion that checks that the maximal intensity values. Maintaining a minimal mode, the algorithm separates the pixels into three groups according to their intensity level. The first group contains the pixels with an intensity greater than or equal to 400 HU (F = 4), the second group the pixels with an intensity greater than or equal to 300 HU (F = 3), and the third group the pixels with an intensity greater than or equal to 200 HU (F = 2). To obtain the resulting F, it is necessary to examine whether the number of pixels in each group maintains the minimal programmed mode; if more than one group meets the sufficient area, the highest density score is considered to be correct; if none of the groups meets the minimal pixel condition, then F = 1 (default value). Once the F values are obtained for each of the proposed methods (F1, F2, F3), a CS is calculated for each F of the selected lesion, and its value is added to the corresponding total CS as indicated in Equation (1).

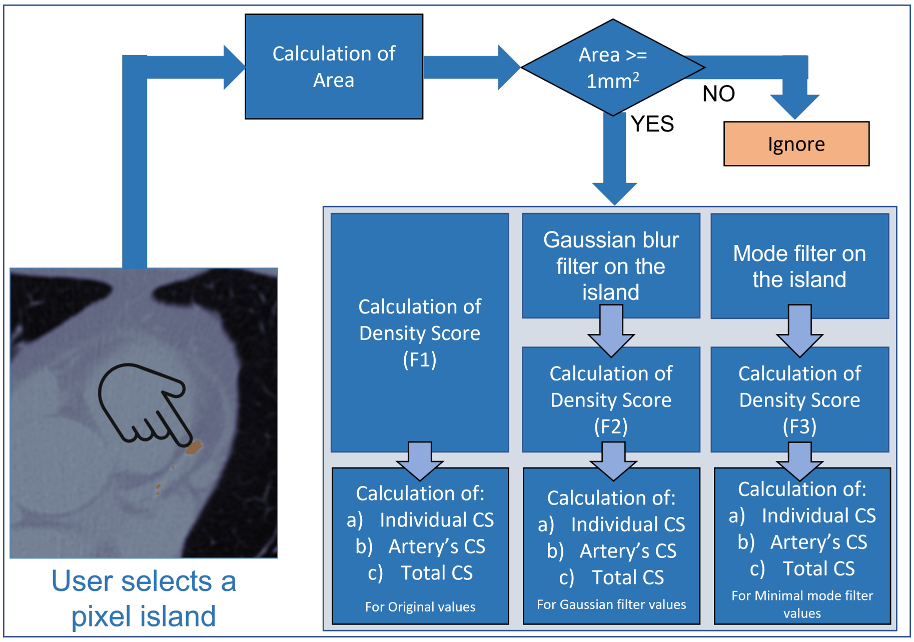

Figure 4. CS calculation flow.

2.4. Validation of Image Processing Calculation Results

To validate the CS calculation proposals, a medical specialist in cardiovascular imaging evaluated CS in each of the studies using the CS plugin of the OsiriX DICOM Viewer software, which is the application he uses daily, and then evaluated the studies selecting the same lesions using the developed image processing tool. The results obtained in the image processing tool are as follows: (1) before applying any processing (Original), (2) after applying the Gaussian filter (Gaussian) to the original image, (3) after applying the minimal mode algorithm (MinMode) to the original image. In this way, the CS results obtained for each density score were compared: (1) OsiriX vs. Original, (2) OsiriX vs. Gaussian, (3) OsiriX vs. MinMode.

2.5. Programming the Web Page and HTTP Requests

The web page was programmed using HTML, CSS, JavaScript, and the Python Flask library. Python is the programming language of the backend of the application, so the Flask instructions allow for transferring the results of image processing and CS calculation to the user interface (frontend) compiled with HTML code and Jinja2 (Used by Flask), in addition to performing traditional HTTP requests (GET or POST). The CSS language is used to define the styles of the page and JavaScript for the interaction and the request of HTTP requests (POST and GET). The requests were through AJAX functions and JSON codes, which allows for the partial and asynchronous updating of the page, obtaining fluency in the interaction. The responses sent by the server are the image resulting from using some of the available functions and the results of the CS calculations. The responses are transferred back using JSON codes again; the resulting JPEG image is encoded with the base64 positional numbering system. The HTTP requests from the application (Figure 5) are the following: (a) increase and decrease the Z position of the set of images. This request helps in navigating through the different slices that the entire CTCS contains. The client performs one of the two GET requests (increase or decrease), and the server modifies the Z position and responds with the corresponding slice image. (b) Activate coronary artery. This is a POST-type request where the client selects the label of the artery with which they want to indicate the lesions. The server receives the selected label and responds with a confirmation, which is reflected in the arteries menu on the web page. (c) Label the calcium lesion. The user can label the lesions by directly selecting the islands of pixels on the image, and the lesion is labeled according to the artery that is active at that moment. The server receives a POST-type request with the X, Y coordinates of the selected pixel, processes the image, performs the CS calculations, and responds to the client with the new image and the obtained results. In addition, a relational database was used for the administration of the users and the CTCS scans uploaded to the application by each of the users. The mysqlclient and SQLAlchemy Python libraries were used for the creation, migration, and updating of the database.

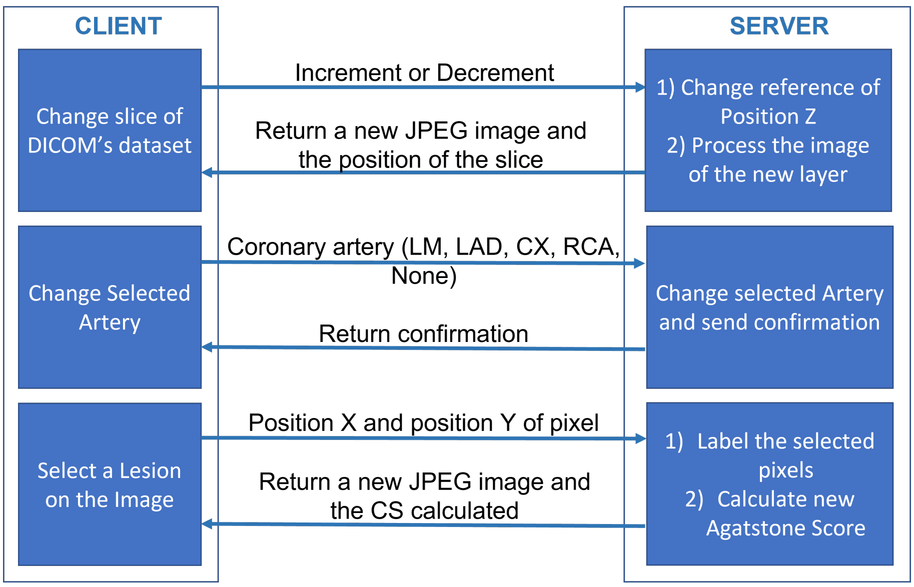

Figure 5. User functions in the web page.

2.6. Setting Up the Application on the Internet

The application was set up on a VPS with Ubuntu 20.04 operating system with NginX services to offer the web service and MariaDB for the database compatible with MySQL.

Using the Python Virtualenv library, a Python 3.8 virtual environment was created with the Pydicom, OpenCV, Flask, and Gunicorn libraries. The used VPS had 4 vCPU cores, 200 GB SSD, and 8 GB of RAM. A system service was activated for the application to have nonstop availability.

3. Results

3.1. CS Calculation and Validation

The diagnoses issued by the specialist were compared with the total CS value per scan for each of the density score calculation methods (Original, Gaussian, MinMode), and the average error was calculated between each of the comparisons, obtaining the following errors: (a) OsiriX vs. Original = 3.8%, (b) OsiriX vs. Gaussian= 4.7%, (c) Osirix vs. MinMode = 1.9%. Another characteristic that was compared was the risk of cardiovascular event corresponding to each of the studies according to the classification given by the CS. Of the 30 studies carried out with the OsiriX software, 7 belonged to the Moderate risk group, 10 to the Moderate–High group, and 13 to the High risk group. The Original function did not correctly classify 1 study as belonging to Moderate–High risk, while the functions with additional processing (Gaussian and MinMode) correctly classified all studies regarding to the results obtained with OsiriX. Figure 6 shows the results of the total CS of each one of the studies where the difference in the results of CS with each of the proposed methods is observed and the limits of the classification by risk of cardiovascular event are also observed.

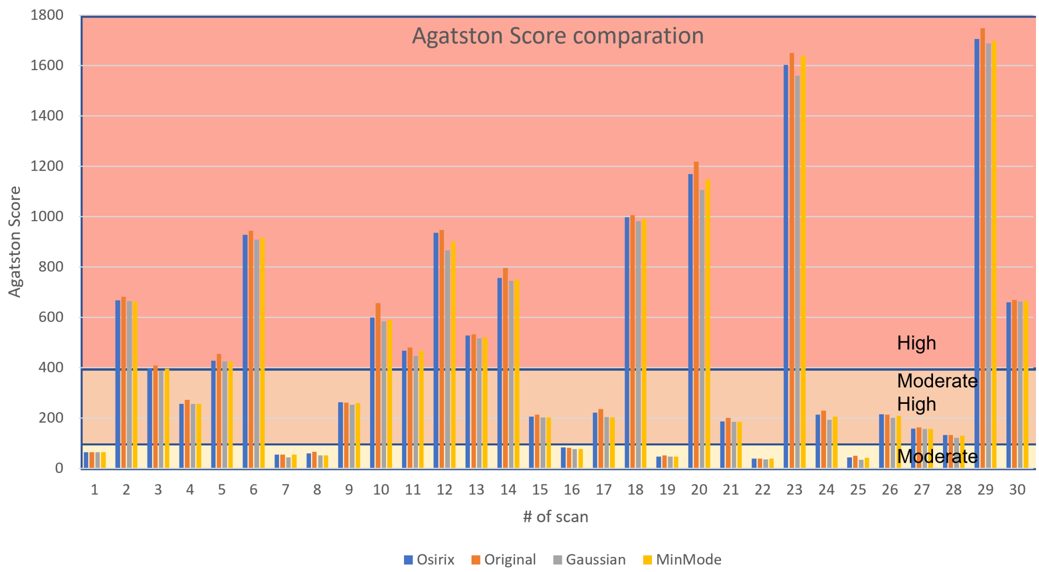

Figure 6. Total CS and risk category classification of the performed studies.

Subsequently, the Pearson's correlation coefficient (r) was calculated for each of the comparisons made, the OsiriX vs. Original comparison obtained r = 0.9996, the OsiriX vs. Gaussian comparison obtained the lowest coefficient with r = 0.9995, and the comparison of OsiriX vs. MinMode r = 0.9997, this being the one with the best correlation of the three.

According to the results obtained in the comparisons of the image processing and CS calculation methods, it is possible to observe that the MinMode technique is the one that most closely resembles the results obtained with the reference commercial software, so this proposal is the one selected to be used in the web application. Figure 7 shows an example on how the results were compared and validated using the same slice from a CTCS scan that had the same pixel area selected. Figure 7a shows the image that was analyzed with Osirix, and the image in Figure 7b was analyzed with the proposed web application.

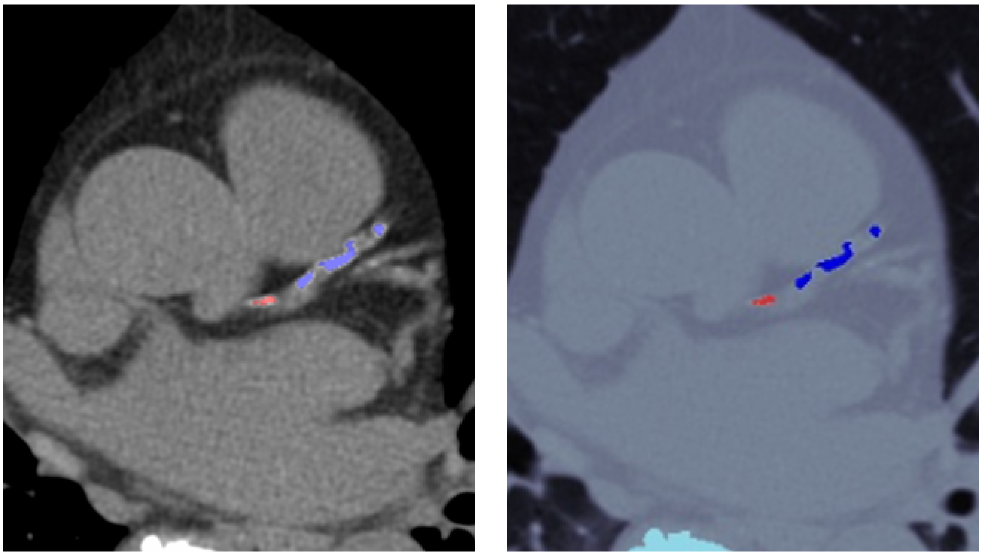

(**a**) (**b**)

Figure 7. Comparison of the same slice from a CTCS scan. (**a**) Image in Osirix Dicom Viewer. (**b**) Image in web application.

3.2. Access to the Web Application

The web application can be accessed from any device with an Internet connection to calculate the CS without the need to have specialized software installed. The proposed application is available to the general public and it has no cost. The application access link is the following: https://www.getcalciumscore.com, accessed on 7 October 2022.

The application has a registration page, as shown in Figure 8; username, e-mail, company, and password data are required. The form shown in Figure 9 is the one corresponding to the login for users who are already registered. Figures 8 and 9 show the main navigation header where the terms and conditions for the use of the application can be reviewed, and the "How to Use" link shows a video explaining the general operation of the web application.

Figure 8. New user registration form.

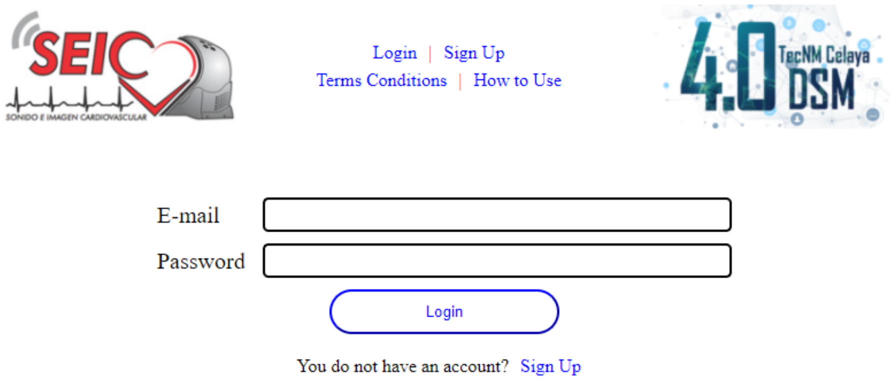

Figure 9. Registered user login form.

Once logged into the application, the user is redirected to the home page (Figure 10), where the option to upload scans is found using the "Upload a new Scan" section, a file in .zip containing a compressed folder with the set of .dcm files. In this section, if no scan is selected, a help image is displayed that indicates the location of each of the tools that the user can use. An exemplary scan is available to all users that does not allow for saving new results or to be eliminated, but it can load results from previously highlighted pixel areas.

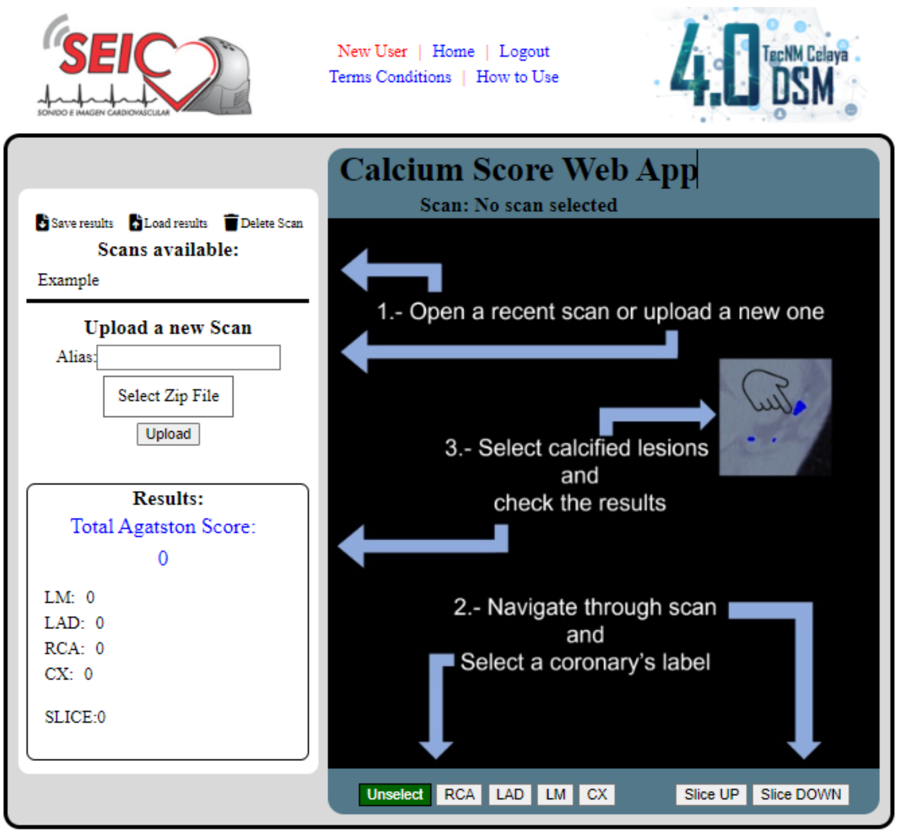

Figure 10. Home page with no scan selected.

The Slice UP and Slice DOWN buttons activate slice change requests and display the previous or next slice, respectively. The "Unselect", "RCA", "LAD", "LM" and "CX" buttons activate requests to change the coronary artery label, the selected label button remains green.

Figure 11 shows the example of the home page where the user has loaded two scans (Patients 1 and 2). Patient 2 is currently selected, and the lesions in the coronary arteries of the entire scan are selected, obtaining a CS of 425 as a result. In Slice 37 (shown in the example), three islands of pixels were selected as CAC lesions in the LAD, one in the LD and one in the CX. The results obtained with the selected islands are saved using the blue "Save results" icon next to the scan name. To load the previously saved results, the green "Load results" icon is used. The red "Delete Scan" icon is used when one wants to remove the scan from the web application; the deleted scans are deleted from the server and from the database. Each of the cyan islands represents the pixels that are above 130 HU (the majority are bones around the chest); they are displayed in this way to assist the user in identifying the ROIs.

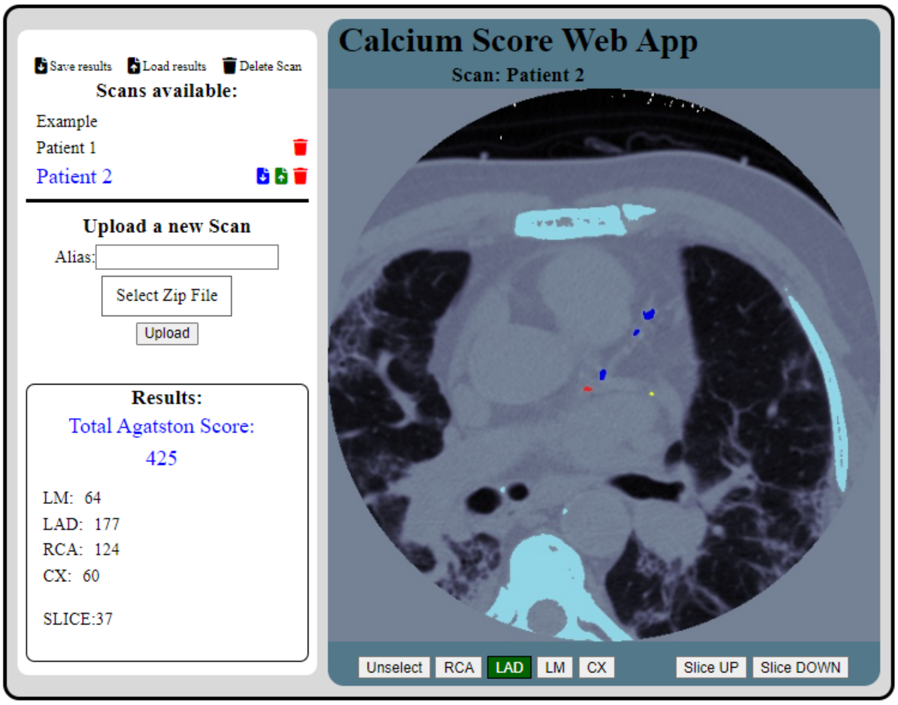

Figure 11. Example of home page with two scans loaded.

4. Discussion

Data comparisons indicate that the results obtained by the proposed web application are like the results obtained with OsiriX DICOM Viewer. The difference between the two tools is attributed to the fact that OsiriX software could use a low-pass filtering technique that is different from the one used in our proposal to reduce variations in the images. Pacsbin (Orion Medical Technologies, Baltimore, MD, pacsbin.com, accessed on 7 October 2022) is a picture archiving and communication system (PACS) that allows for viewing DICOM images; with support for the most common image manipulation tools, its main contribution is to bring a fully featured PACS environment to the web for teaching cases and research. Recent articles [45–47] mentioned the importance of Pacsbin in distance learning in the training of future radiologists, which is possible because it was developed as a web-based system. Although Pacsbin is an application with multiple image analysis tools, it does not allow for the measurement of calcium in coronary arteries like the web application proposed in this article.

Marco Aiello [48] provided a comparative table of the 10 DICOM viewers used in their study. The evaluated software can read and display DICOM images, and all are free-access or open-source; some paid software was included if a free trial version was available. Of the 10 listed programs, only two could be used from a web browser (Postdicom and Papaya Viewer), and two allow for calculating the CS (Horos Viewer, 3D slicer), but they do not meet both characteristics. In other web applications related to CS [49,50], statistical studies of patients with CAC were carried out, and calculators that estimate the percentage derived from the age, sex, ethnicity and CS of the patient were proposed, so the application suggested in this article complements this type of tools used by physicians.

5. Conclusions

In this study, a web application for the quantification of CS was implemented. Three measurements were proposed: (1) without using any additional processing for variations in the image, (2) using a Gaussian blur filter to attenuate the noise generated in the CTCS, and (3) using an algorithm that ensures a minimal number of pixels with the same density score. The data were compared against commercial software OsiriX DICOM Viewer where the third applied algorithm had a higher correlation (r = 0.9997). The average error that was obtained for the CS comparison in the proposal without filter was 3.8%,4.7% for the proposal with Gaussian filter, and 1.9% for the minimal mode algorithm.

Of the studies, 96% for the original proposal and 100% using any of the proposed filtering algorithms were correctly classified in the corresponding risk group. The implementation of some additional processing to reduce noise in the image and thus have more stable HU values was considered to be important. This proposal offers a web application available from any device with Internet access and a web browser to perform the interpretation and calculation of the calcium score in the coronary arteries without the need for installing additional software. The medical specialist who supported the development of this application found it to be a notable and very useful tool that facilitates the calculation of the calcium score from any device and without the need for a specific DICOM viewer. He found that the application was not complicated in its operation, it was very intuitive, and that further it simplified the selection of calcified areas by having the high intensity areas marked before marking them. The clinical cardiologist would be able to elaborate, consult, and compare studies of their patients at any time. Lastly, it facilitates cardiologists or other medical specialists in interacting with one of the tools that is gaining the most acceptance worldwide in the prevention of cardiovascular risk.

Author Contributions: Conceptualization, J.A.-A. and S.O.-T.; methodology, J.A.-A. and J.M.-N.; software, J.A.-A. and J.P.-M.; validation, S.O.-T. and J.M.-N.; formal analysis, S.O.-T.; investigation, V.S.-O., M.B.-S. and J.P.-M.; resources, S.O.-T.; writing—review and editing, V.S.-O. and M.B.-S.; supervision, J.M.-N.; project administration, J.M.-N. All authors have read and agreed to the published version of the manuscript.

Funding: This research received no external funding.

Institutional Review Board Statement: Not applicable.

Informed Consent Statement: Not applicable.

Data Availability Statement: Not applicable.

Acknowledgments: This research did not receive any specific grant from funding agencies in the public, commercial, or not-for-profit sectors.

Conflicts of Interest: The authors declare no conflict of interest.

References

1. World Health Organization. Cardiovascular Diseases. Fact Sheet. 2021. Available online: https://www.who.int/news-room/fact-sheets/detail/cardiovascular-diseases-(cvds) (accessed on 10 July 2022).
2. Lusis, A.J. Atherosclerosis. *Nature* **2000**, *407*, 233–241. [CrossRef] [PubMed]
3. Patel, J.; Blaha, M.J.; McEvoy, J.W.; Qadir, S.; Tota-Maharaj, R.; Shaw, L.J.; Rumberger, J.A.; Callister, T.Q.; Berman, D.S.; Min, J.K.; et al. All-cause mortality in asymptomatic persons with extensive Agatston scores above 1000. *J. Cardiovasc. Comput. Tomogr.* **2014**, *8*, 26–32. [CrossRef] [PubMed]
4. Hecht, H.S. Coronary Artery Calcium and Prevention Guidelines. *JACC Cardiovasc. Imaging* **2020**, *13*, 1187–1190. [CrossRef] [PubMed]
5. Greenland, P.; LaBree, L.; Azen, S.P.; Doherty, T.M.; Detrano, R.C. Coronary Artery Calcium Score Combined With Framingham Score for Risk Prediction in Asymptomatic Individuals. *JAMA* **2004**, *291*, 210–215. [CrossRef] [PubMed]

6. Taylor, A.J.; Bindeman, J.; Feuerstein, I.; Cao, F.; Brazaitis, M.; O'Malley, P.G. Coronary Calcium Independently Predicts Incident Premature Coronary Heart Disease Over Measured Cardiovascular Risk Factors: Mean Three-Year Outcomes in the Prospective Army Coronary Calcium (PACC) Project. *J. Am. Coll. Cardiol.* **2005**, *46*, 807–814. [CrossRef]
7. Shaw, L.J.; Raggi, P.; Schisterman, E.; Berman, D.S.; Callister, T.Q. Prognostic Value of Cardiac Risk Factors and Coronary Artery Calcium Screening for All-Cause Mortality. *Radiology* **2003**, *228*, 826–833. [CrossRef]
8. Isgum, I.; Bartels-Rutten, A.; Prokop, M.; Ginneken, B. Detection of coronary calcifications from computed tomography scans for automated risk assessment of coronary artery disease. *Med. Phys.* **2007**, *34*, 1450–1461. [CrossRef]
9. Agatston, A.S.; Janowitz, W.R.; Hildner, F.J.; Zusmer, N.R.; Viamonte, M.; Detrano, R. Quantification of coronary artery calcium using ultrafast computed tomography. *J. Am. Coll. Cardiol.* **1990**, *15*, 827–832. [CrossRef]
10. Palomares, J.F.; Evangelista, A. Cuantificación del calcio aórtico y arteriosclerosis vascular en individuos asintomáticos: más allá de las arterias coronarias. *Rev. Esp. Cardiol.* **2016**, *69*, 813–816. [CrossRef]
11. Yoon, W.J.; Crisostomo, P.; Halandras, P.; Bechara, C.F.; Aulivola, B. The use of the Agatston calcium score in predicting carotid plaque vulnerability. *Ann. Vasc. Surg.* **2019**, *54*, 22–26. [CrossRef]
12. 3D Slicer Image Computing Platform. Available online: https://www.slicer.org/ (accessed on 10 July 2022).
13. Kay, F.U.; Abbara, S.; Joshi, P.H.; Garg, S.; Khera, A.; Peshock, R.M. Identification of high-risk left ventricular hypertrophy on calcium scoring cardiac computed tomography scans: validation in the DHS. *Circ.Cardiovasc. Imaging* **2020**, *13*, e009678. [CrossRef] [PubMed]
14. Foldyna, B.; Eslami, P.; Scholtz, J.E.; Baltrusaitis, K.; Lu, M.T.; Massaro, J.M.; D'Agostino, R.B.; Ferencik, M.; Aerts, H.J.; O'Donnell, C.J.; et al. Density and morphology of coronary artery calcium for the prediction of cardiovascular events: insights from the Framingham Heart Study. *Eur. Radiol.* **2019**, *29*, 6140–6148. [CrossRef] [PubMed]
15. Dransfield, M.T.; Huang, F.; Nath, H.; Singh, S.P.; Bailey, W.C.; Washko, G.R. CT emphysema predicts thoracic aortic calcification in smokers with and without COPD. *COPD.* **2010**, *7*, 404–410. [CrossRef]
16. Image Processing and Analysis in Java. Available online: https://imagej.nih.gov/ij/index.html (accessed on 10 July 2022).
17. Sun, Z.; Ng, C.K. High calcium scores in coronary CT angiography: effects of image post-processing on visualization and measurement of coronary lumen diameter. *J. Med. Imaging. Health. Inform.* **2015**, *5*, 110–116. [CrossRef]
18. Phillips-Eakley, A.K.; McKenney-Drake, M.L.; Bahls, M.; Newcomer, S.C.; Radcliffe, J.S.; Wastney, M.E.; Van Alstine, W.G.; Jackson, G.; Alloosh, M.; Martin, B.R.; et al. Effect of high-calcium diet on coronary artery disease in Ossabaw miniature swine with metabolic syndrome. *J. Am. Heart. Assoc.* **2015**, *4*, e001620. [CrossRef]
19. Cahalane, R.M.; Broderick, S.P.; Kavanagh, E.G.; Moloney, M.A.; Mongrain, R.; Purtill, H.; Walsh, M.T.; O'Brien, J.M. Comparative analysis of calcification parameters with Agatston Score approximations for ex vivo atherosclerotic lesions. *J. Cardiovasc. Comput. Tomogr.* **2020**, *14*, 20–26. [CrossRef]
20. Bos, D.; Ikram, M.A.; Elias-Smale, S.E.; Krestin, G.P.; Hofman, A.; Witteman, J.C.; van der Lugt, A.; Vernooij, M.W. Calcification in major vessel beds relates to vascular brain disease. *Arterioscler. Thromb. Vasc. Biol.* **2011**, *31*, 2331–2337. [CrossRef]
21. OpenCV. Available online: https://opencv.org/ (accessed on 10 July 2022).
22. Durlak, F.; Wels, M.; Schwemmer, C.; Sühling, M.; Steidl, S.; Maier, A. Growing a random forest with fuzzy spatial features for fully automatic artery-specific coronary calcium scoring. In *International Workshop on Machine Learning in Medical Imaging*; Springer: Berlin/Heidelberg, Germany, 2017; pp. 27–35. [CrossRef]
23. Toji, B.; Ohmiya, J.; Kondo, S.; Ishikawa, K.; Yamamoto, M. Fully Automatic Extraction of Carotid Artery Contours from Ultrasound Images. *IEICE Trans. Inf. Syst.* **2014**, *97*, 2493–2500. [CrossRef]
24. Mirunalini, P.; Aravindan, C.; Nambi, A.T.; Poorvaja, S.; Priya, V.P. Segmentation of Coronary Arteries from CTA axial slices using Deep Learning techniques. In Proceedings of the TENCON 2019—2019 IEEE Region 10 Conference (TENCON), Kochi, India, 17–20 October 2019; pp. 2074–2080. [CrossRef]
25. de Vos, B.D.; Wolterink, J.M.; Leiner, T.; de Jong, P.A.; Lessmann, N.; Išgum, I. Direct automatic coronary calcium scoring in cardiac and chest CT. *IEEE Trans. Med. Imaging* **2019**, *38*, 2127–2138. [CrossRef]
26. Garousi, V.; Mesbah, A.; Betin-Can, A.; Mirshokraie, S. A systematic mapping study of web application testing. *Inf. Softw. Technol.* **2013**, *55*, 1374–1396. [CrossRef]
27. Verber, D.; Novak, D.; Borovič, M.; Dugonik, J.; Flisar, D. EQUIDopa: A responsive web application for the levodopa equivalent dose calculator. *Comput. Methods Programs Biomed.* **2020**, *196*, 105633. [CrossRef]
28. Al-Waisy, A.S.; Alruban, A.; Al-Fahdawi, S.; Qahwaji, R.; Ponirakis, G.; Malik, R.A.; Mohammed, M.A.; Kadry, S. CellsDeepNet: A Novel Deep Learning-Based Web Application for the Automated Morphometric Analysis of Corneal Endothelial Cells. *Mathematics* **2022**, *10*, 320. [CrossRef]
29. Pemmaraju, R.; Minahan, R.; Wang, E.; Schadl, K.; Daldrup-Link, H.; Habte, F. Web-Based Application for Biomedical Image Registry, Analysis, and Translation (BiRAT). *Tomography* **2022**, *8*, 1453–1462. [CrossRef]
30. Mora-Aguilera, G.; Martínez-Bustamante, V.; Acevedo-Sánchez, G.; Coria-Contreras, J.J.; Guzmán-Hernández, E.; Flores-Colorado, O.E.; Mendoza-Ramos, C.; Hernández-Nava, G.; Álvarez-Maya, I.; Gutiérrez-Espinosa, M.A.; et al. Surveillance web system and mouthwash-saliva qPCR for labor ambulatory SARS-CoV-2 detection and prevention. *Int. J. Environ. Res. Public Health* **2022**, *19*, 1271. [CrossRef]
31. Villavicencio, C.N.; Macrohon, J.J.; Inbaraj, X.A.; Jeng, J.H.; Hsieh, J.G. Development of a Machine Learning Based Web Application for Early Diagnosis of COVID-19 Based on Symptoms. *Diagnostics* **2022**, *12*, 821. [CrossRef]

32. Lanera, C.; Azzolina, D.; Pirotti, F.; Prosepe, I.; Lorenzoni, G.; Berchialla, P.; Gregori, D. A Web-Based Application to Monitor and Inform about the COVID-19 Outbreak in Italy: The {COVID-19ita} Initiative. *Healthcare* **2022**, *10*, 473. [CrossRef]
33. Nawi, N.A.M.M.; Sapiai, N.S.; Ghazali, S.A.M.; Rusok, N.H.M.; Zulkifli, F.Z.; Mazlan, F.M. Developing an E-College Monitoring System as a Web-Based Monitoring Tool Application. *Proceedings* **2022**, *82*, 25. [CrossRef]
34. Mejía, S.; Muñoz, I.C.; Serna, L.Y.; Sarmiento, C.A.; Bravo, C.L.; Hernández, A.M. Web Applications for Teaching the Respiratory System: Content Validation. *Appl. Sci.* **2022**, *12*, 4289. [CrossRef]
35. Udias, A.; Pistocchi, A.; Vigiak, O.; Grizzetti, B.; Bouraoui, F.; Alfaro, C. ESPRES: A web application for interactive analysis of multiple pressures in aquatic ecosystems. *Sci. Total Environ.* **2020**, *744*, 140792. [CrossRef] [PubMed]
36. Andreo-Martínez, P.; Ortiz-Martínez, V.M.; Muñoz, A.; Menchón-Sánchez, P.; Quesada-Medina, J. A web application to estimate the carbon footprint of constructed wetlands. *Environ. Model Softw.* **2021**, *135*, 104898. [CrossRef]
37. Cochard, T.; Branger, M.; Supply, P.; Sreevatsan, S.; Biet, F. MAC-INMV-SSR: a web application dedicated to genotyping members of Mycobacterium avium complex (MAC) including Mycobacterium avium subsp. paratuberculosis strains. *Infect. Genet. Evol.* **2020**, *77*, 104075. [CrossRef] [PubMed]
38. Karatzas, E.; Baltoumas, F.A.; Kasionis, I.; Sanoudou, D.; Eliopoulos, A.G.; Theodosiou, T.; Iliopoulos, I.; Pavlopoulos, G.A. Darling: A Web Application for Detecting Disease-Related Biomedical Entity Associations with Literature Mining. *Biomolecules* **2022**, *12*, 520. [CrossRef] [PubMed]
39. Bianchetti, G.; Abeltino, A.; Serantoni, C.; Ardito, F.; Malta, D.; De Spirito, M.; Maulucci, G. Personalized Self-Monitoring of Energy Balance through Integration in a Web-Application of Dietary, Anthropometric, and Physical Activity Data. *J. Pers. Med.* **2022**, *12*, 568. [CrossRef]
40. Cubillas, J.J.; Ramos, M.I.; Jurado, J.M.; Feito, F.R. A Machine Learning Model for Early Prediction of Crop Yield, Nested in a Web Application in the Cloud: A Case Study in an Olive Grove in Southern Spain. *Agriculture* **2022**, *12*, 1345. [CrossRef]
41. Paraschiv, L.S.; Acomi, N.; Serban, A.; Paraschiv, S. A web application for analysis of heat transfer through building walls and calculation of optimal insulation thickness. *Energy Rep.* **2020**, *6*, 343–353. [CrossRef]
42. Mason, D. SU-E-T-33: pydicom: An open source DICOM library. *Med. Phys.* **2011**, *38*, 3493–3493. [CrossRef]
43. Pulli, K.; Baksheev, A.; Kornyakov, K.; Eruhimov, V. Real-time computer vision with OpenCV. *Commun. ACM* **2012**, *55*, 61–69. [CrossRef]
44. Nelson, J.C.; Kronmal, R.A.; Carr, J.J.; McNitt-Gray, M.F.; Wong, N.D.; Loria, C.M.; Goldin, J.G.; Williams, O.D.; Detrano, R. Measuring coronary calcium on CT images adjusted for attenuation differences. *Radiology* **2005**, *235*, 403–414. [CrossRef]
45. McRoy, C.; Patel, L.; Gaddam, D.S.; Rothenberg, S.; Herring, A.; Hamm, J.; Chelala, L.; Weinstein, J.; Smith, E.; Awan, O. Radiology education in the time of COVID-19: a novel distance learning workstation experience for residents. *Acad. Radiol.* **2020**, *27*, 1467–1474. [CrossRef]
46. Awan, O.A.; Klein, J.S. Stepping Up to the Challenge: Overcoming Barriers to Radiology Training in the United States During COVID-19. *Can. Assoc. Radiol. J.* **2021**, *72*, 11–12. [CrossRef]
47. Sugi, M.D.; Kennedy, T.A.; Shah, V.; Hartung, M.P. Bridging the gap: interactive, case-based learning in radiology education. *Abdom. Radiol.* **2021**, *46*, 5503–5508. [CrossRef] [PubMed]
48. Aiello, M.; Esposito, G.; Pagliari, G.; Borrelli, P.; Brancato, V.; Salvatore, M. How does DICOM support big data management? Investigating its use in medical imaging community. *Insights Imaging* **2021**, *12*, 1–21. [CrossRef] [PubMed]
49. de Ronde, M.W.; Khoshiwal, A.; Planken, R.N.; Boekholdt, S.M.; Biemond, M.; Budoff, M.J.; Cooil, B.; Lotufo, P.A.; Bensenor, I.M.; Ohmoto-Sekine, Y.; et al. A pooled-analysis of age and sex based coronary artery calcium scores percentiles. *J. Cardiovasc. Comput. Tomogr.* **2020**, *14*, 414–420. [CrossRef] [PubMed]
50. McClelland, R.L.; Chung, H.; Detrano, R.; Post, W.; Kronmal, R.A. Distribution of coronary artery calcium by race, gender, and age: results from the Multi-Ethnic Study of Atherosclerosis (MESA). *Circulation* **2006**, *113*, 30–37. [CrossRef]